

Construction of a Current Controller to Study the Interactions of ${}^6\text{Li}$ and ${}^{133}\text{Cs}$ at Ultralow Temperatures

Peter Scherpelz

Cheng Chin, Advisor

James Franck Institute and Department of Physics, University of Chicago

June 3, 2009

We aim to study the interactions between lithium and cesium atoms in a magneto-optical trap and an optical dipole trap. In particular, we will study the dependence of the collision properties on the external magnetic field and identify Feshbach resonances between the two species. Here I present the design and testing of the current controller used to drive the magnetic coil and access the Feshbach resonances. An operational feedback-stabilized circuit to drive currents up to 200 A is presented, and the performance and errors of the feedback loop are analyzed. With modest improvements, it should be possible to drive two coils at 250 A each.

1 Introduction and Background

Interactions between cesium and lithium, which include inelastic collisions, elastic collisions, and the creation of bound molecular states, are interesting for at least four reasons. First, to study lithium and cesium at ultracold temperatures and especially in degeneracy, inelastic collision losses from the trap must be minimized. Second, elastic scattering can influence the performance of sympathetic cooling, which may aid in bringing lithium to degeneracy through its collisions with the typically colder cesium atoms.

Third, bound molecular states may be of fundamental physical interest. One use of ultracold atomic systems is as a model system for more complex quantum phenomena, such as high-temperature superconductivity or quantum chromodynamics. The ability to create and study bound molecular states in this controlled system is therefore extremely important as it opens up a richer set of systems to study. For example, a pairing gap related to superfluidity has been observed using Feshbach resonances with ultracold lithium [1]. Finding different molecular states of lithium and cesium should provide other opportunities for exploring physical theories.

Finally, by loading both lithium and cesium into optical lattices, we hope to perform scalable quantum information processing by using the cesium atoms as messengers between lithium qubits [2]. Realizing this scheme, however, necessitates the implementation of controlled quantum gates,

which require a coupling between the lithium and cesium atoms. A weakly bound molecular state could provide this desired coupling.

Weakly bound molecular states are the result of Feshbach resonances, which occur at specific magnetic field strengths [3]. The resonances for cesium and lithium are quite different, with cesium having sharper resonances at smaller magnetic field strengths. Similarly, mixing lithium and cesium may lead to new Feshbach resonances, which would be correlated with currently unknown molecular states. This study necessitates building a controller, presented below, for our magnetic field coils. With the controller, we can seek Feshbach resonances over a large range of field strengths.

1.1 Previous Work with Bosonic Lithium

Some of the above phenomena have been explored with ${}^7\text{Li}$ and ${}^{133}\text{Cs}$ [4, 5, 6]. Early experiments used a magneto-optical trap to evaluate the interspecies collision properties. In these studies the excited Li state repelled the ground-state Cs state, so these interactions did not result in trap losses. Ground-state Li, however, can inelastically collide with excited Cs to produce trap losses. If both species are in the ground state, the dynamics present do not result in trap loss until the lithium trap depth is below about 9 GHz, at which point hyperfine collisions are significant [4].

The group went on to study collisions in a dipole trap. They were able to detect the sympathetic cooling of lithium, as well as hyperfine interactions that can result in trap loss [5, 6]. However, we expect many of these interactions to change with ${}^6\text{Li}$. Furthermore, Feshbach resonances are also isotope specific, and were not studied in these experiments.

2 Current Controller Construction

2.1 Motivation

Our experiment to study interactions between lithium and cesium requires a magnetic field for two purposes. First, the atoms are initially trapped in a magneto-optical trap (MOT). This MOT requires a magnetic field gradient on the order of 15 G/cm. To reach this magnetic field gradient, we have two magnetic coils, which must have current driven through them in opposite directions. In this anti-Helmholtz coil configuration, the center between the two coils will have a linear magnetic field gradient in all three spatial directions. To reach a gradient of 15 G/cm, currents of about 10 A are necessary.

Second, to reach Feshbach resonances, specific magnetic field strengths must be present at the location of the atoms. In this case, the atoms are transferred from the MOT into an optical dipole trap, so a magnetic field gradient is no longer necessary or desirable. Among the Feshbach resonances we hope to access, there is one broad resonance for ${}^6\text{Li}$ at about 834 G [3]. Here the coils must be driven with current in the same direction, also called a Helmholtz configuration, displayed in Figure 1. In this configuration, 1 Ampere driven through both coils provides about a 4 G magnetic field

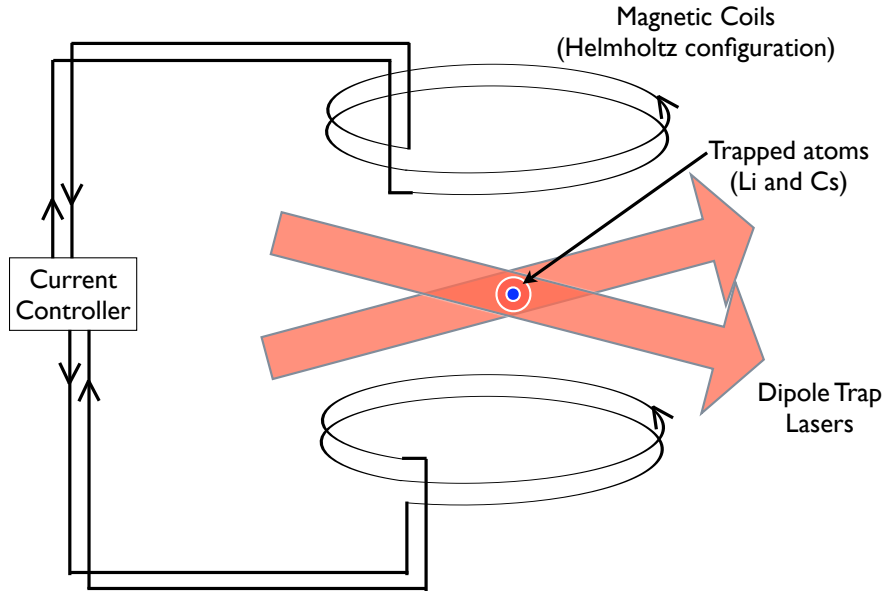


Figure 1: A diagram demonstrating the use of the current controller in the experimental setup. Here, the atoms are trapped in a dipole trap, and the two coils are used to produce a magnetic field that affects the scattering properties of the trapped atoms. The current controller is used to output a stable current to the two coils.

at the position of the atoms. To reach the desired field of 1000 G (in order to access both sides of the actual resonance), a current of 250 A must be driven through each coil.

Furthermore, to use these resonances, we need to be able to access specific magnetic fields and maintain a stable field, as otherwise the scattering properties of the atoms will drift as the magnetic field drifts. We hope to achieve a stability of at least 1 part in 10^4 , which would translate to 0.1 G stability. However, even better stabilities would be preferable in order to maintain very stable scattering lengths close to the resonance.

To achieve these goals, we need a device which will provide stable currents through each coil up to at least 250 A. In order to access both an anti-Helmholtz field configuration and a Helmholtz configuration, the current direction through at least one coil needs to be reversible. This project is to construct and test a current source that satisfies these requirements.

2.2 Controller Design

To change the current direction through the coil, we have adopted the design sketched in Figure 2, copied for the two coils. This setup provides for smoothly changing the direction of current through a coil by moving from $I_U - I_L > 0$ to $I_U - I_L < 0$.

Sensing the voltage across the shunt resistor in Figure 2 provides the input to a feedback loop, whose purpose and design is presented in Section 2.3. The feedback circuit then outputs two currents, $I_{M1} = I_o + I_{FB}$ and $I_{M2} = I_{o'} - I_{FB}$, where I_o and $I_{o'}$ are bias currents set by potentiometers

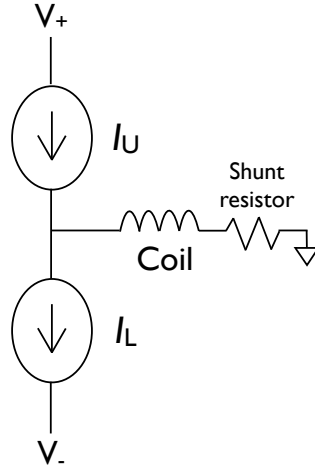


Figure 2: A diagram of the current controller framework. The current sources I_U and I_L are controlled by one feedback loop. The voltage across the shunt resistor is read by the feedback circuits to adjust the difference in current between I_U and I_L . The inductor symbols are taken from <http://en.wikiboks.org/wiki/File:Inductor.svg>.

while I_{FB} is a current set by the feedback loop. We then use current mirrors with a gain G to set

$$\begin{aligned} I_U &= GI_{M1} = GI_o + GI_{FB} \\ I_L &= GI_{M2} = GI_{o'} - GI_{FB}. \end{aligned} \quad (1)$$

The gain G is necessary here as I_{M1} and I_{M2} are limited by the feedback circuit design to at most a few Amperes. Thus, to reach 250 A, significant gain must be provided, which is accomplished with a mirror using n-channel field effect transistors, described in Section 2.4.

From equation (1), it can be seen that the difference in currents, $I_U - I_L$, is equal to $GI_o - GI_{o'} + 2GI_{FB}$. Thus, the current through the coil is simply the feedback current times some large gain, with a small constant offset due to the bias currents that is corrected automatically by virtue of the feedback mechanism.

To implement this circuit, three major components are required. First, the feedback circuits must be built. Second, each current I_{M1} or I_{M2} above must be mirrored with gain G . Third, the actual current sources must be constructed to handle the high currents required.

2.3 Feedback and Control Circuit

There are two primary reasons for using a feedback circuit. First, it provides increased stability compared to an open-loop mechanism, which is necessary considering the requirement of 1 part in 10^4 current stability in order to reduce magnetic field noise and drift, which in turn would otherwise cause variation in the scattering properties of the atoms. Second, the gain G above is strongly dependent on the temperature and drain-source voltages of the transistors that are used to

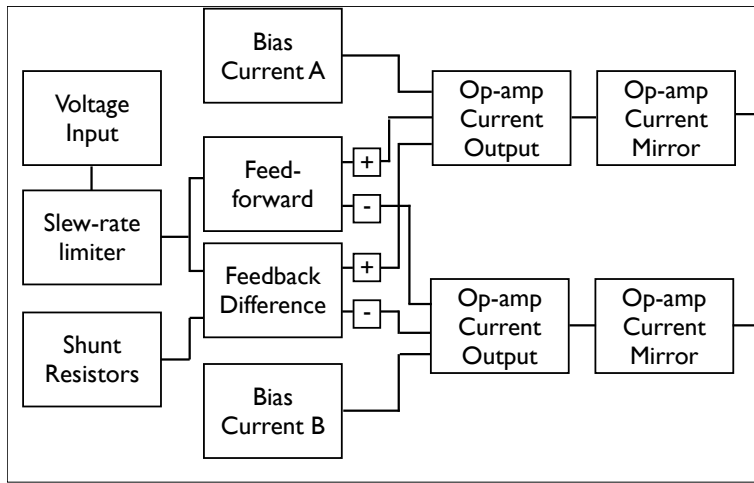


Figure 3: A block diagram of the control circuit. The voltage input is first limited in its slew rate to prevent sudden voltage changes from interfering with the feedback response. This slew rate-limited input is compared to the voltage measured across the shunt resistors to generate the error signal, which is then integrated and sent to the current output as the feedback control. In addition, the input is also delivered directly to the current outputs to improve the speed and allow operation with the feedback loop disabled. Two potentiometers control the constant bias currents. Finally, the current output signal is mirrored with about ten times gain to produce a current output up to about 2 A.

provide the high current. As a result, without a feedback mechanism, it would be extremely difficult to achieve any sort of stability or repeatability in current settings, as it would depend strongly on the temperature of the transistors and the current being driven through the coil (which affects the drain-source voltage of the transistors).

The block diagram of the control circuit is presented in Figure 3, based upon a circuit design by Nate Gemelke. Each current output is determined by a constant bias current, set with a potentiometer, a feedforward voltage input, allowing fast response times, and a feedback input, which is ultimately responsible for the stability of the system. The feedforward and feedback inputs are sent to the two current outputs with opposite signs, resulting in the proper currents for I_{M1} and I_{M2} , above.

This circuit has been tested in its entirety, with the exception of an on/off switch that will be connected to water flow and temperature sensors to provide automatic shutoff before the circuit overheats. All parts of the circuit functioned properly during testing, except for the current mirror. This was initially implemented with an APEX PA12 power operational amplifier in the inverting configuration displayed in Figure 4.

However, this configuration created oscillation in both this stage and the previous current output stage of the circuit at about 400 kHz. Adding capacitors to slow down circuit components or varying the output load could bring the oscillation down to below 10 kHz but could not eliminate the oscillation. We then switched to a non-inverting current mirror, displayed in Figure 5, which eliminated the oscillation.

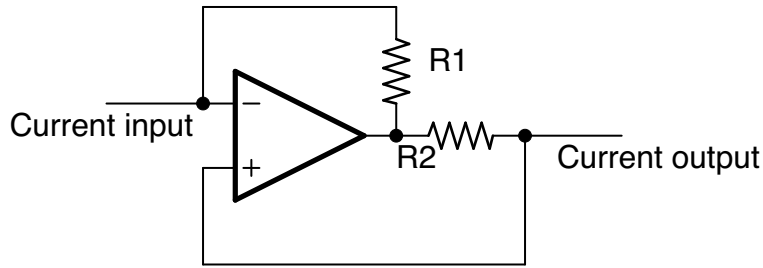


Figure 4: A diagram of the inverting current mirror originally used in the control circuit. The current gain in this circuit is $-R1/R2$. We used $R1 = 10 \Omega$ and $R2 = 1 \Omega$.

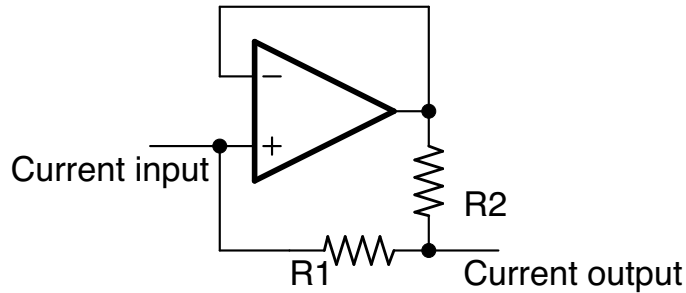


Figure 5: The non-inverting current mirror we are now using in the control circuit. The current gain in this circuit is $1 + R1/R2$. We again used $R1 = 10 \Omega$ and $R2 = 1 \Omega$.

2.4 Current Mirrors

As the feedback circuit only provides currents of a few Amperes at most, there must be a stage that mirrors these currents into the current of at least 250 A required for the magnetic coils. This stage is constructed using n-channel field-effect transistors (FETs). A FET is a device in which an electric field, determined by the voltage between the gate and source terminals, sets the conductivity and thus the current through a doped semiconductor channel. As a result, the gate-source voltage sets the current between the source and drain terminals. N-channel FETs will have a current that flows into the drain and exits from the source.

The overall schematic of the current mirrors is displayed in Figure 6. We are using an IRF510 n-channel FET for the low-power side that accepts current from the feedback circuit's output. This FET is paired with the high-power IXFN340N07 FET, which can supply as much as 100 A of current at DC operation and a voltage across the drain and source of 6 V. These two FETs have similar curves of drain-source current versus the gate-source voltage. As a result, the current input to the IRF510 defines a current across the IXFN340N07 FET which is much larger but approximately linearly related.

This n-channel mirror was tested for stability and speed in isolation from the rest of the circuit. A current output using a PA12 op-amp was provided to the IRF510 FET, and the n-channel mirror

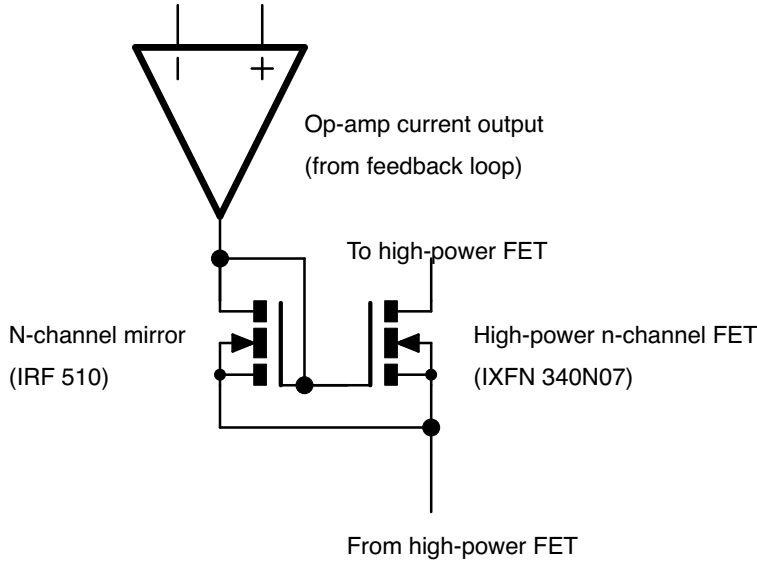


Figure 6: The diagram of the current mirrors using field-effect transistors. By selecting FETs with an appropriate gate-source threshold voltage $V_{GS(th)}$, the n-channel mirrors then provide a large amount of gain that is constant over most of the current range.

was constructed as in Figure 6. A magnetic coil was added in series with the current input to provide inductance and simulate the final setup. The transfer function was then measured with a spectrum analyzer. This system was tested at different temperatures up to 68°C and was stable. It was also tested at total current outputs up to 40 A for one FET and was stable.

One critical factor in the speed of the n-channel mirrors is sufficient drain-source voltage for the high-current FET, both due to slew rate and capacitance limitations. The slew rate for current is limited by $dI/dt \leq V/L$ where V is the supply voltage for the high current path and L is the series inductance from the magnetic coil. However, most of the transfer functions should not have been affected by this factor as only the small signal response, and thus very small current changes, were probed. Instead, the capacitance of the FET increases as the voltage across its drain and source decreases, leading to a further slowing of the circuit, which was observed here. Figure 7 shows the effect of decreasing supply voltage in this situation. Note that increasing the inductance of the coil will similarly slow the mirror.

A second critical factor, also relating to the capacitance of the FETs, is the number of FETs in parallel. We hope to use five IXFN340N07 FETs in parallel for each current source, due to the 250 A requirement on their output at a unit duty cycle. Two FETs were tested in parallel here. Indeed, the response slowed significantly compared to one FET, as shown in Figure 8.

Overall, the supply voltage is the critical factor in determining the response. At high currents, the voltage drop across the magnetic coil increases, so the total supply voltage must increase to supply the same voltage drop across the FETs. Similarly, as the number of FETs increases the supply voltage must increase to combat the increased total capacitance of the system. These factors

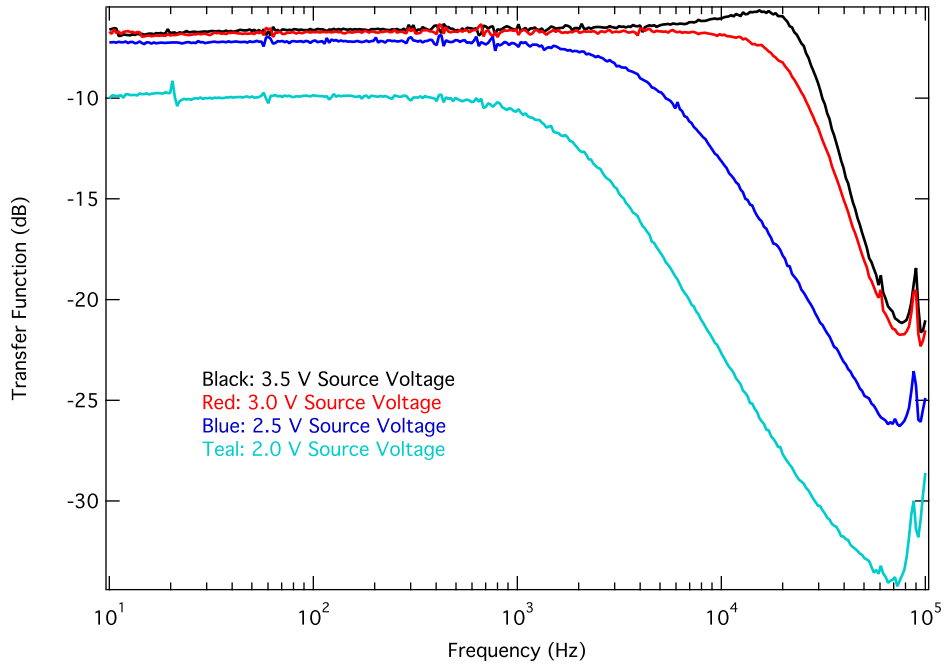


Figure 7: The dependence of the transfer function on the supply voltage, which is the sum of the voltage across the drain and source of the high-current FET and the voltage across the magnetic coil. Here a 15-turn coil with $L \approx 15 \mu\text{H}$ was used. The current across the IRF510 low-current FET was 0.38 A, resulting in about 20 A through the high-current IXFN340N07 FET. In the graph above, as supply voltage decreases, the 3 dB point decreases from 30.4 kHz to 2.2 kHz. The peak in the top curve is probably due to an LC resonance.

must be weighed against the heatsinking capability of the system, as a voltage increase translates to a proportional increase in power dissipation for the FETs, as explained below.

2.5 Heat Dissipation

The heat dissipation requirements of this circuit are determined by the bias currents across the power FETs. At zero current through the coil and power supplies at $\pm V$ above and below ground, each set of FETs will dissipate $I_B V$ power. With four sets of FETs, the total power dissipation at zero current through the coil will be $4I_B V$. This is the highest power dissipation experienced during operation, because when current runs through the coil, there is a significant voltage drop across the coil and less total power is dissipated in the FETs due to the decreased voltage across the FETs with the larger current passing through them. For a bias current of 125 A (the minimum required to reach 250 A total, assuming a symmetric and constant gain), and $V = 6$ Volts, the power dissipation is 3 kW. For more overhead in the voltage and current available for the circuit, a bias current of 175 A and $V = 7$ Volts could be used, which gives 4.9 kW total power dissipation. To accomplish this, a heatsink was designed and constructed, and is presented in Figure 9. It is a 6" \times 6" \times 1" copper block with four 0.375"-diameter bores through which chilled water is pumped. The thermal

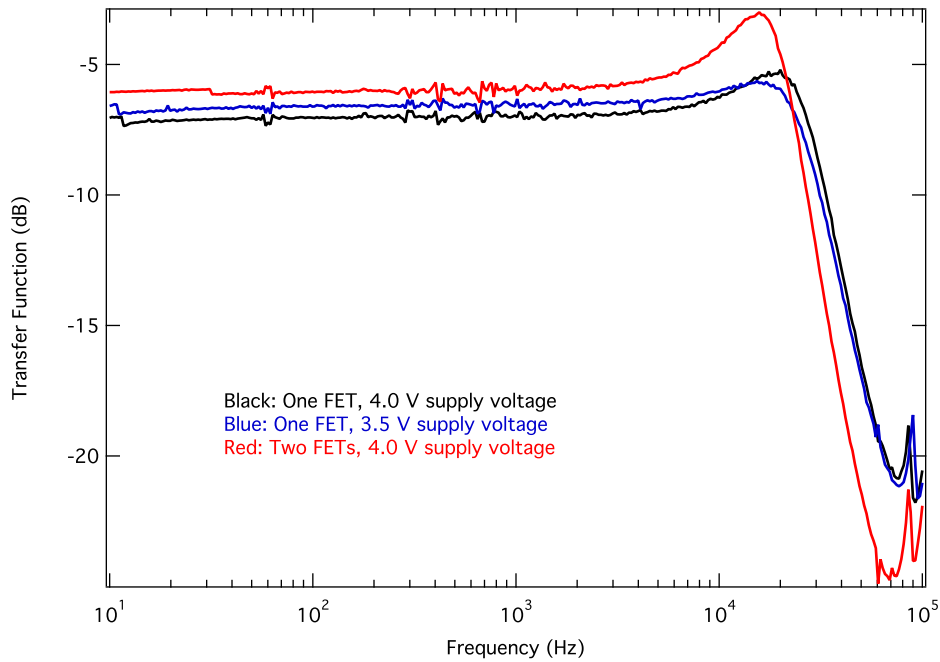


Figure 8: The dependence of the transfer function on the number of FETs. The input current to the IRF510 was 0.38 A in all of these curves. Output current was about 20 A for the single FET and 24 A for the two FETs (demonstrating the two mirrors do not have identical gain, which may be a concern in the future). Both 4.0 V and 3.5 V supply voltages are included for one FET, as the drain-source voltage changes some for two FETs due to the larger total current, and thus larger voltage, through the magnetic coil. The drain-source voltage for the data with two FETs should lie somewhere between the two drain-source voltages for the single FET curves, and overall the 3 dB point for the two FETs is 4 to 6 kHz lower than for a single FET. Also note the higher resonant peak, probably also due to the increased capacitance of the two-FET system.

resistance of this setup was tested at 200 A bias current and 7 V supply voltage through two sets of FETs. This is 2800 W of power dissipation, and resulted in a 53 degree heatsink temperature, with the circulating water heated to about 25° C. Thus, the thermal resistance of the heatsink is about 0.01 K/W, which is consistent with measurements at lower levels of power dissipation. The thermal resistance of each FET is quoted as 0.23 K/W from the FET junction to the heatsink, which means in this test each FET may have reached about 117° C junction temperature, compared to an absolute maximum temperature of 150° C junction temperature the FETs are rated for.

To allow higher total power dissipation, two additional heatsink blocks have been fabricated that will attach to the main heatsink used here. Water will flow between the heatsinks, providing more surface area between the water and copper with which to dissipate heat. These heatsinks have not yet been tested.

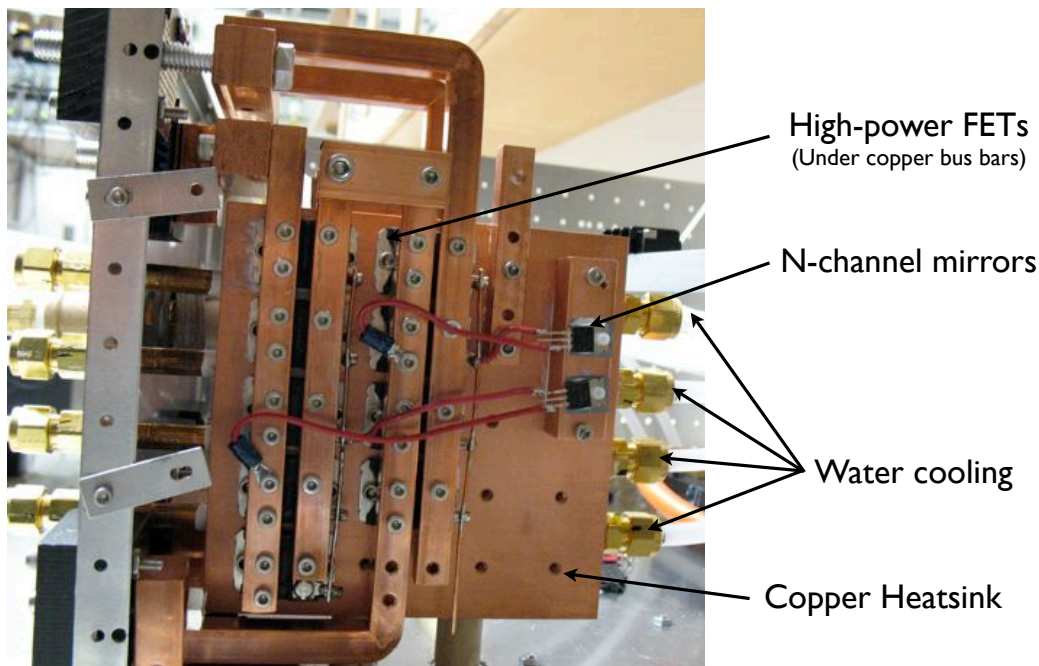


Figure 9: A picture of the heatsink and mounting system. Four water lines run through the heatsink to cool it. Ten FETs (nine shown here) are mounted on each side of the heatsink, as well as the other n-channel mirror FETs on the right.

2.6 Feedback Circuit

The feedback circuit is constructed by placing a $0.5\text{ m}\Omega$ shunt resistor in series with each magnetic coil. The voltage across this resistor is amplified using a Texas Instruments INA103 instrumentation amplifier. The output of this amplifier is then subtracted from the input voltage in an INA111 instrumentation amplifier, forming the error signal. Finally, after a potentiometer which allows adjusting the gain of the feedback loop, one operational amplifier in an OP470 chip is used to integrate the error signal. This integrated signal is then sent to the current stages of the circuit (see Figure 3). A schematic of this feedback mechanism is presented in Figure 10.

In the performance of the feedback circuit, we are interested primarily in performance at the unity gain point. As frequency increases, the open-loop gain of the feedback circuit will decrease, and at some point it will go from above one to below one. If at any frequency below this point the phase shift between the input voltage and the feedback reaches π , the system will oscillate. If, at the unity gain point, the phase shift is close to π , there will be a spike in the noise at this point, but actual oscillation will not necessarily occur. If the system is well below unity gain, the peak should be negligible.

The feedback circuit must be configured with two primary criteria. First, the error needs to be suppressed at low frequencies. This suppression will be stronger the larger the gain. Second, the system needs to be stable so that it will not enter oscillation during its operation. This is especially important in this circuit, as large and potentially dangerous heating can occur through oscillating currents in the magnetic coil. To balance these two criteria, an FFT of the noise spectrum was

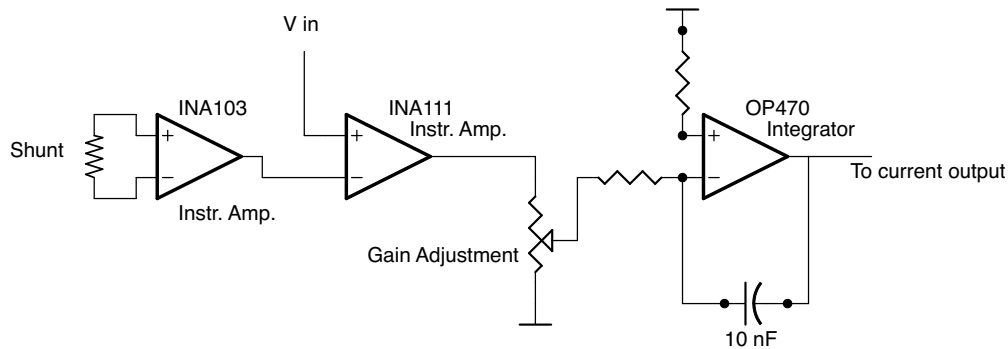


Figure 10: The diagram of the feedback section of the control circuit. The shunt resistor is amplified with a ten times gain by the INA103, and the voltage input into the circuit is then subtracted from this output to form an error signal. Finally, the signal is integrated and sent to the op-amp current output in the circuit.

taken at various gain settings, both with the feedback loop turned on and with it off. Two of these spectra are displayed in Figure 11. The unity gain point was found to be about 3 kHz. This value is fairly low, and prevents strong noise suppression. This low unity gain point is probably due to the very large capacitance of the FETs, as well as the inductance of the coil, which both slow down the circuit as a whole. However, even with this unity gain point, noise suppression can be observed at low frequencies.

2.7 Circuit Performance

2.7.1 Errors in Feedback Signal

To analyze the performance of the feedback circuit, in addition to the transfer functions above, it is also important to evaluate the sources of error in the feedback circuit itself, which limit the accuracy of the error signal and thus the overall noise suppression of the circuit. The absolute calibration of the magnetic field and current will be done using the atoms, so systematic errors that result in permanent offsets in the feedback loop, such as input offsets in amplifiers, do not need to be considered. However, errors that cause the current to change during operation are important. These include random error, such as input noise in amplifiers, and systematic errors, such as errors due to heating of the shunt resistor.

The most significant errors are related to the performance of the shunt resistor and the instrumentation amplifiers at different temperatures. First, the shunt resistor is rated to a 15 ppm/°C change in resistance due to heating. If we assume a 3° variation in temperature over normal operation, this means slow drifts of up to 45 ppm in the feedback calibration are possible. Note this temperature variation may be due both to the 30 W heating on each of two resistors, as well as variations in the water temperature itself. The resistors are cooled using water supplied in parallel with the large heatsink, but the lab water reservoir temperature may still be impacted by the overall

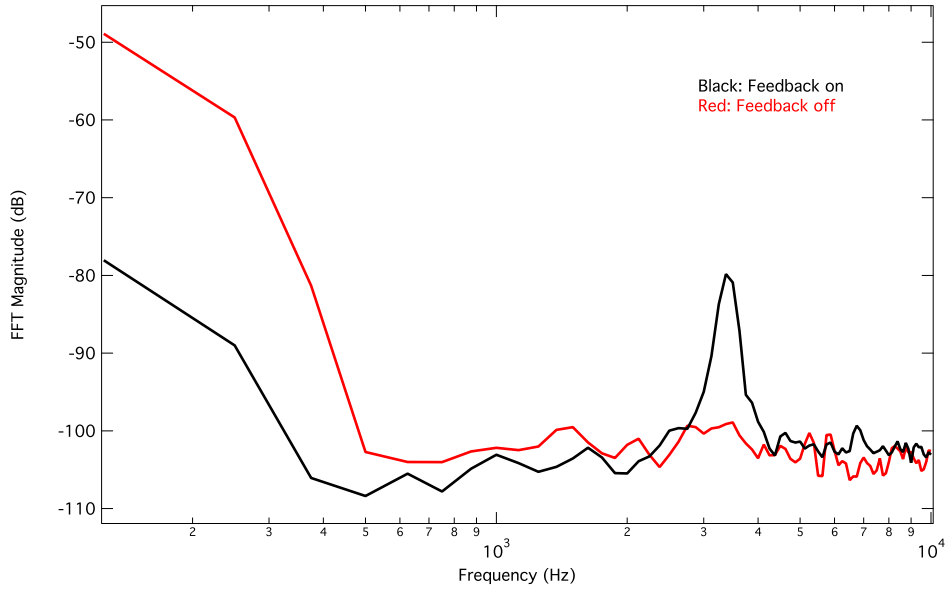


Figure 11: The FFT of the error signal, which is the shunt resistor signal after its amplification minus the input voltage. Here the input voltage is zero, and the bias is set for about 24 A to run through each FET current source I_U and I_L . This graph shows that the noise at low frequencies is suppressed by 0.5 to 3 orders of magnitude due to the feedback, but there is a peak at about 3.4 kHz seen only when feedback is on, which is due to increased feedback gain near the open-loop unity gain point. This graph represents the upper limit of gain possible while still avoiding oscillation; the gain may be reduced some for actual operation to ensure circuit stability.

heat load.

Second, the INA103 instrumentation amplifier has a gain nonlinearity of 25 ppm/ $^{\circ}\text{C}$. The heating on these chips should be less than on the shunt resistors. If we estimate it as about 0.2°C due both to internal heating and ambient heating, this is a 5 ppm variation. In addition, there is input voltage offset drift of $3\mu\text{V}/^{\circ}\text{C}$. We expect a nominal 125 mV signal in the input of the INA103, so at 0.2°C this is a 5 ppm effect. Input noise is negligible compared to these effects at 1 to 2 nV/ $\sqrt{\text{Hz}}$. Finally, the common-mode error is also negligible. If we assume about 0.5 m Ω resistance from the shunt resistor to ground, the two shunt resistor connections are biased around 190 mV above ground. With more than 75 dB CMR through 3 kHz, only about 6 nV error should be present.

The INA111 has similar errors due to heating. Common-mode rejection error is about 10 times larger, and input noise is a factor of 10 larger as well, but these errors are still negligible compared to heating error. The errors are tabulated in Table 1. Overall, a 54 ppm drift is expected with these parameters, largely due to heating of the shunt resistor. In the future, this stability will be measured using Hall-effect current sensors to provide independent current measurements.

2.7.2 Slew Rate

The slew rate is primarily limited by the inductance of the coil. We measured the coil inductance of our test coil by acquiring the transfer function of a simple series LC circuit with a known capacitance.

Table 1: Errors present in the feedback loop. Note that integrated circuit errors due to temperature drifts are not added in quadrature because they are not independent.

Error source	Quoted error value	Estimated actual error at 0.2°C
Shunt resistor: (Canadian Shunt THB-400-200) Temperature coeff. of resistance	15 ppm/°C	45 ppm (at 3°C)
INA103:		
Gain nonlinearity	25 ppm/°C	5 ppm
Input offset drift	3 μ V/°C	5 ppm
Input noise	2 nV/ $\sqrt{\text{Hz}}$	< 1 ppm
Common-mode error	75 dB CMR	< 1 ppm
INA11:		
Gain nonlinearity	10 ppm/°C	2 ppm
Input offset drift	100 μ V/°C	16 ppm
Input noise	13 nV/ $\sqrt{\text{Hz}}$	< 1 ppm
Common-mode error	65 dB CMR	< 1 ppm
OP470:		
Input offset drift	2 μ V/°C	2 ppm
Total:		54 ppm

The inductance was found to be about 14 μ H. This is similar to the final coils we will use, which were measured to have inductances of 5 and 10 μ H. For the test coil, we will have at most 7 V through the coil and the FETs to drive current changes. Thus, at best we can generate current slew rates of about $V/L = 4 \times 10^5$ A/s through the coil.

The actual slew rate starting at 0 A and slewing to 40 A through the coil was found using a square wave input to the feedback loop with a function generator, and then using an oscilloscope to measure the output of the INA103 instrumentation amplifier (which is simply an amplified copy of the voltage across the shunt resistor). The oscilloscope output is shown in Figure 12. As only a 4 V input was used here, 3×10^5 A/s would be the highest possible slew rate. The observed slew rate of about 1.5×10^5 A/s is about half this, which is indicative of the approximately 2 V the FETs need to operate within saturation mode.

2.7.3 Nonlinear Gain at High Coil Currents

One remaining problem with the circuit performance is the nonlinear gain of the apparatus due to voltage changes at high currents through the coil. When starting at 200 A bias current, and power supplies biased at ± 7 V about ground, each n-channel mirror requires an input of about 0.5

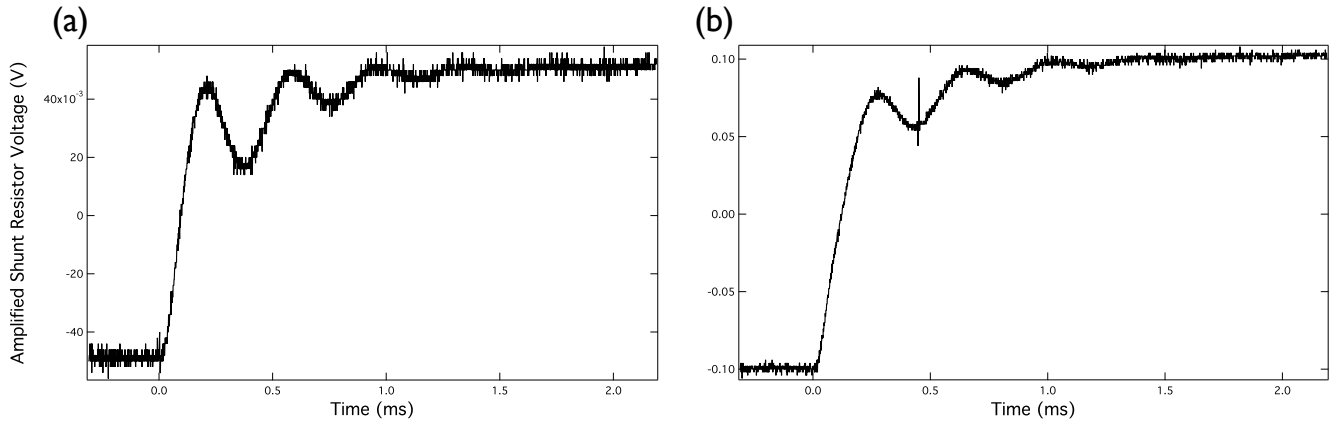


Figure 12: Two oscilloscope traces of the response to a square wave. **(a)** shows the response to a 100 mV amplitude, 10 Hz square wave input, creating a -10 A to +10 A output current. **(b)** shows the response to a 200 mV amplitude, 10 Hz square wave input, which generates a -20 A to +20 A current. The voltage is measured from the INA103 output, which gives the voltage across the shunt resistor with ten times gain.

A. To provide 200 A current into the coil, the input currents change to 0.9 A and 0.15 A, which correspond to currents of 227 A and 25 A. Notice that changing the input to I_L from 0.5 A to 0.15 A changed the current I_L from 200 A to 25 A, whereas changing the input to I_U from 0.5 A to 0.9 A brought the 200 A I_U current up to only 227 A. The problem is that only difference currents of about 230 A can be reached with this asymmetric gain, as once I_L reaches 0, the feedback circuit does not operate properly.

The reason for this asymmetric change is that as the current through the coil (equal to $I_U - I_L$, as in Section 2.2) increases, the voltage drop across the upper bank of FETs generating I_U drops significantly, changing the gain curve so that an input current of much greater than 0.9 A would be required to generate the desired $I_U = 250-300$ A.

The planned solution to this is to add in a potentiometer to allow asymmetric inputs to the mirrors. Thus, if the two inputs are biased to 0.5 A each, one would rise to 1.3 A output or more while the other only dropped to, suppose, 0.2 A, helping to make the actual gain more linear and thus reach difference currents above the required 250 A before I_L reaches zero.

At this point, the current controller has successfully been tested beginning with a ± 7 V supply, 200 A bias current through both I_U and I_L , and subsequently generating a 230 A difference current through the coil. With the simple modification of asymmetric gain, and improved heat dissipation, this current controller should be capable of operating two coils at 250 A each.

3 Conclusion

I have designed, constructed, and tested a current controller for outputting large amounts of current necessary to generate magnetic fields used to trap atoms and manipulate the scattering properties

of those atoms. This circuit includes a feedback circuit to provide long-term stability and decreased noise in the current output, current mirrors to achieve the high currents required, and significant water-cooling apparatuses for the heat dissipation required.

The feedback circuit has been tested and shown to reduce noise. It has a unity gain point of about 3 kHz, which allows moderate noise suppression at low frequencies. The long-term stability of the feedback loop is primarily dependent on the temperature stability of the shunt resistor and feedback circuitry, but the stability is estimated to be within 50 ppm under moderate temperature drifts.

This circuit has been tested at 2800 W power dissipation, and feedback-stabilized currents through a test coil of 230 A were achieved. The slew rate of this circuit was measured as 1.5×10^5 A/s, which should be able to be increased at higher operating voltages. The remaining challenges are to fix the nonlinear gain of the system as the current through the coil is increased, and to improve the heatsinking mechanism to dissipate the 3 to 5.5 kW of power dissipation expected when both coils are being used.

4 Acknowledgements

Thanks to Nate Gemelke for the circuit board design and his assistance in all aspects of the project. Thanks as well to Kuo-Tung Lin for his help machining.

References

- [1] Chin, C. *et al.* Observation of the Pairing Gap in a Strongly Interacting Fermi Gas. *Science* **305**, 1128–1130 (2004).
- [2] Brickman Soderberg, K.-A., Gemelke, N. & Chin, C. Ultracold molecules: vehicles to scalable quantum information processing. *New Journal of Physics* **11**, 055022 (2009).
- [3] Chin, C., Grimm, R., Julienne, P. & Tiesinga, E. Feshbach Resonances in Ultracold Gases. *ArXiv e-prints* (2008). 0812.1496.
- [4] Schlöder, U., Engler, H., Schünemann, U., Grimm, R. & Weidemüller, M. Cold inelastic collisions between lithium and cesium in a two-species magneto-optical trap. *The European Physical Journal D-Atomic, Molecular and Optical Physics* **7**, 331–340 (1999).
- [5] Mosk, A. *et al.* Mixture of ultracold lithium and cesium atoms in an optical dipole trap. *Applied Physics B: Lasers and Optics* **73**, 791–799 (2001).
- [6] Mudrich, M. *et al.* Sympathetic Cooling with Two Atomic Species in an Optical Trap. *Physical Review Letters* **88**, 253001 (2002).